Rock and Soil Mechanics

Volume 41 | Issue 1 Article 13

9-23-2020

Research on karst cavity detection method based on multi-frequency borehole sonar

Jin-chao WANG

Chuan-ying WANG

Xin-jian TANG

Zeng-qiang HAN

See next page for additional authors

Custom Citation

WANG Jin-chao, WANG Chuan-ying, TANG Xin-jian, HAN Zeng-qiang, WANG Yi-teng, HU Sheng. Research on karst cavity detection method based on multi-frequency borehole sonar[J]. Rock and Soil Mechanics, 2020, 41(1): 353-360.

Research on karst cavity detection method based on multi-frequency borehole sonar

Authors

Jin-chao WANG, Chuan-ying WANG, Xin-jian TANG, Zeng-qiang HAN, Yi-teng WANG, and Sheng HU

Rock and Soil Mechanics 2020 41(1): 353−360 ISSN 1000−7598
https: //doi.org/10.16285/j.rsm.2018.7340 rocksoilmech.researchcommons.org/journal

Research on karst cavity detection method based on multi-frequency borehole sonar

WANG Jin-chao, WANG Chuan-ying, TANG Xin-jian, HAN Zeng-qiang, WANG Yi-teng, HU Sheng
State Key Laboratory of Geomechanics and Geotechnical Engineering, Institute of Rock and Soil Mechanics, Chinese Academy of Sciences, Wuhan, Hubei 430071, China

Abstract: The shape and size characteristics of underground cavity are of great significance to the stability calculation and evaluation of geological structure in the region. However, the borehole sonar currently used lacks universality and it is difficult to meet the requirements of both detection accuracy and detection range. Therefore, on the basis of traditional borehole sonar method, this paper proposes a new method of detecting cavity based on multi-frequency borehole sonar. With considerations given to the contribution of different frequencies to the actual detection object, this method synthesizes the detection data of various frequencies and effectively solves the problem of the opposition between detection scale and detection accuracy. Firstly, the optimal frequency expression of the detection system is derived to provide basic parameters to reflect the influence of different frequencies on the analysis of detection results to a greater extent, and the frequency influence factor parameter is established to describe the deviation degree between the natural frequency and the optimal frequency. Then, on the basis of superposition of the frequency influence factor, the detection data of various detection frequencies are synthesised, and detection objects are accurately measured by using the improved spectrum ranging method. Finally, after adding depth and azimuth information, the three-dimensional reconstruction of cavity shape is realized. The feasibility and accuracy of the method are verified by applying it to practical engineering projects.

Keywords: borehole sonar; multi-frequency sonar; cavity shape; cavity size; underground detection

1 Introduction

China is one of the countries that have the most extensive karst development in the world. With a total area of 3.46 million square kilometres, accounting for 1/3 of the land area[1-2]. The karst areas in China are most widely distributed in Guangxi, Guizhou and the eastern part of Yunnan. Western Hunan, Western Hubei, Eastern Sichuan, Shandong, Shanxi and other places are also rich in karst development[3]. With the natural water stored in karst being a rich water resource, karst caves can also play important roles in the development of tourism, energy reserves and so on. Therefore, it is of great significance to carry out engineering construction, land consolidation, environmental protection, development and utilization of the water resources, mineral resources, and tourism resources in areas of karst distribution. Karst develops as a kind of natural phenomenon with diverse distribution and peculiar form. However, contributing by the complexity, uncertainty and concealment of karst, it can also be a potential geological hazard[4], which may endanger the safety of buildings, reservoirs, mines, and other facilities, even cause ground subsidence and damage to the ecological environment, and have a certain impact on the project construction. Therefore, it is necessary to investigate the karst and understand its development and distribution law before commencing engineering construction in karst distribution area.

In karst exploration, because of the heterogeneity of karst space development and the complexity of its hydrogeological conditions, it is difficult to obtain satisfactory results only by traditional geological methods. It is therefore usually reasonable to carry out karst exploration using geological method in combination with other exploration methods. Conventional geophysical exploration methods of karst exploration include high density apparent resistivity method, traditional seismic reflection method, ground penetrating radar method, advanced drilling method, elastic wave CT method, pipe wave test method, etc. [5-12]. However, in the calculation and evaluation of the karst cave roof stability, the size and contour of the cave should also be considered. If the plane distribution of the cave is larger than the width of the cave roof foundation, the stability of the cave roof will be worse. Moreover, the more irregular the shape of the cave, the more concentrated the stress and the worse the stability of the cave roof[13]. However, it is difficult to reflect the size and outline of the karst cave with high accuracy by the currently used geophysical prospecting method.

At present, the widely used cavity sonar in water-soluble salt caverns can effectively measure the size and contour of underground caverns. However, due to the shape irregularity and scale uncertainty of the naturally formed underground caverns, it is difficult to measure the size and contour of the natural caverns by directly applying the cavity sonar.

Received: 12 December 2018 Revised: 28 April 2019
This work was supported by the National Natural Science Foundation of China (41731284); the Young Foundation of the National Natural Science of China (No.41902294).
First author: WANG Jin-chao, male, born in 1988, PhD, assistant Professor, mainly engaged in the research of underground space exploration and geotechnical testing.E-mail: jcwang@whrsm.ac.cn

Therefore, established on the traditional cavity sonar, this paper proposes a cave detection method based on multi frequency borehole sonar. By setting up multiple sonar probes, the influence of different frequencies on the detected object is considered, and the influence of different frequencies on the detection results analysis is, to a greater extent, preferentially reflected, so that the contradiction between detection scale and detection accuracy can be effectively avoided. This allows the exploration system to better adapt to the detection of caves subjected to shape irregularity and size uncertainty, providing favorable data support for the engineering construction in karst areas.

2 Borehole sonar detection technology

Borehole sonar detection technology mainly uses sonar measurement technology to realize the detection of cave shape. Its main working principle is to lower the sonar probe into the cave, and the transmitting transducer on the sonar probe will send directional sound wave to the surrounding rock wall. The transmitting sound wave will be reflected by the rock wall and then received by the receiving transducer on the sonar probe. The horizontal distance between the sonar probe and the rock wall will be calculated by analysing the time of transmitting and receiving the sound wave signal. When the rotation of the sonar probe is one circle, the distance between the sonar probe and the rock wall at a certain depth can be measured, and the description of the omni-directional shape of the karst cave can be achieved by constantly lowering the sonar probe into the cave.

The structure and principle diagram of the drilling sonar detection system is shown in Fig.1. The sonar probe mainly includes sonar transmitting/receiving transducer, rotary motor, electronic compass, probe circuit and transmission cable, etc. The system components on the ground include depth winch, power/signal control box, communication line and computer with measuring depth [14].

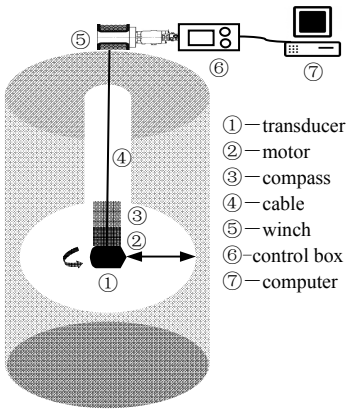

Fig.1 System structure diagram

The sonar probe equipped with the transmitting/receiving transducer, rotation motor, electronic compass and other components, is vertically suspended in the borehole through the cable. The cable is connected with the winch which measures the depth. The depth winch is connected with the control box on the ground, and the control box is connected with the computer to realize the real-time display and storage of the karst cave outline. The sonar probe is vertically lowered through the depth winch, which obtains the profile data of the horizontal section at various depths of the underground karst cave. The transmitting/receiving transducer driven by the rotation motor rotates horizontally to realize the horizontal section scanning of the karst cave rock wall. The profile of horizontal section of the karst cave can be correctly obtained according to the position of the transmitting/receiving transducer and distance fitting of the measuring points. Depth data can be obtained according to the length of cable lowered by the depth winch inside of the borehole. The profile data of each section and the corresponding depth data are transmitted to the computer at the same time. According to the depth of the transmitting/receiving transducer, the horizontal profile curves of each section are spliced to form the three-dimensional profile of the cave, so as to realize the detection of the size and profile of the cavity.

3 Multi-frequency sonar detection method

Because of the irregular shape and uncertain scale of the natural underground karst cave, it is difficult to measure the size and contour of the natural karst cave by directly applying the traditional borehole sonar detection technology. In view of the particularity of underground natural karst caves, a multi-frequency sonar detection method is proposed.

3.1 Establishment of optimum frequency function

In different detection environments, the optimal detection frequency of acoustic signal is different. If the size of the detection object is large, the detection frequency should be smaller in order to reduce the acoustic attenuation. On the other hand, if the size of the detection object is small, and the reflection of the detection object is good, the detection frequency is usually higher in order to obtain higher detection accuracy. In the detection of karst caves, to simultaneously satisfy the requirements of detection accuracy and detection range, the best detection frequency should be selected according to the real-time situation, so the optimal detection result in a specific detection environment can be achieved.

In the drilling sonar detection system, the active echo detection method is usually used for measurement. The difference of the medium of the detection environment is relatively small, but the shape and size of the caves vary significantly. Therefore, when using the drilling sonar technology to detect the cave, this paper mainly considers the influence of the detection distance on the selection of the sonar frequency, and establishes an optimum frequency function $\overline{f}(r)$ based on the detection distance. If the distance of the detected object remains unchanged, the optimum frequency of the transmitting/receiving transducer in the drilling sonar detection system can be deduced according to the quality factor F_{M}, which is defined as

$$F_{\mathrm{M}} = S_{\mathrm{L}}^{\ 4} / (N_{\mathrm{L}} - D_{\mathrm{I}} + D_{\mathrm{T}}) \tag{1}$$

where S_{L} is the sound source level of the sonar probe; N_{L} is the noise level of the surrounding environment of the sonar probe; D_{I} is the receiving directivity index of the sonar probe; D_{T} is the detection threshold of the sonar probe.

The specific form of the optimum frequency depends on the calculation result of $\mathrm{d}F_{\mathrm{M}} / \mathrm{d}f$. In order to ensure a fixed beam angle, the receiving directivity index D_{I} is taken as a constant, that is, it is independent of frequency. It is assumed that the receiving bandwidth is proportional to the operating frequency, i.e. $\Delta f = Kf$. The radiation power is constant. The detection threshold is independent of the frequency, i.e.

$$\frac{\mathrm{d}S_{\mathrm{L}}}{\mathrm{d}f} = \frac{\mathrm{d}D_{\mathrm{I}}}{\mathrm{d}f} = \frac{\mathrm{d}D_{\mathrm{T}}}{\mathrm{d}f} = 0 \tag{2}$$

When the frequency changes one octave and the change rate of noise level N_{L} is -3 dB, the optimum frequency function $\overline{f}(r)$ is

$$\overline{f}(r) = \frac{11.6}{r^{2/3}} \tag{3}$$

where r is the working distance (km) between the sonar probe and the detection object. According to the relation (3), when the action distance r is 1−10 m, the optimum frequency $\overline{f}$ is 1.2 MHz−250 kHz.

In the detection of karst caves, because the detection scale is unknown, it is difficult to accurately obtain the action distance r between the sonar probe and the detection object. However, in order for the working frequency of sonar to approximate the best detection frequency, the estimated action distance $\tilde{r}$ can be used to calculate the optimal frequency $\overline{f}$ of sonar, and the change of frequency is one octave. The change rate of noise level is -3dB, so the optimum frequency function of drilling sonar can be expressed as

$$\overline{f}(\tilde{r}) = \frac{11.6}{\tilde{r}^{2/3}} \tag{4}$$

where: $\tilde{r}$ is the estimated detection distance between the cave wall and the probe, which can be obtained from geological data or sonar equipment.

3.2 Determination of frequency influence factor

In order for the sonar transducer to work at the optimum frequency, the sonar transducer needs to be in a broadband mode. At present, manufacturing wide-band high-power sonar transducer is not only costly but also associated with some technical problems. In addition, it requires high-level matching between the transducer and power amplifier. On the other hand, sonar transducer in the narrow-band mode has easier control and higher accuracy over the selection and switching of the working frequency in comparison with the wide-band mode sonar transducer. Therefore, the method described in this paper can replace the wide-band sonar transducer by arranging multiple narrow-band sonar transducers with different natural frequencies. In order to better meet the detection requirements, the concept of parameter of frequency influence factor is introduced.

The parameter of frequency influence factor is used to express the distance between the natural frequency and the optimum frequency of the narrow-band sonar transducer. The larger the parameter value, the smaller the deviation between the natural frequency and the optimum frequency of the transducer, and the maximum value is infinitely close to one, while the smaller the parameter value, the larger the deviation between the natural frequency and the optimum frequency of the transducer, and the minimum value is infinitely close to zero. Assuming that n transducers are uniformly arranged on the sonar probe, the frequency influence factor α_i corresponding to the i-th narrow-band sonar transducer can be expressed as

$$\alpha_i = \frac{\left(\left|f_1 - \overline{f}\right| + \ldots + \left|f_{i-1} - \overline{f}\right| + \left|f_{i+1} - \overline{f}\right| + \ldots + \left|f_n - \overline{f}\right|\right)}{(n-1)\left(\left|f_1 - \overline{f}\right| + \ldots + \left|f_i - \overline{f}\right| + \ldots + \left|f_n - \overline{f}\right|\right)} \tag{5}$$

In the formula, f_1, f_2, ... f_{n-1} and f_n are the natural frequencies corresponding to the narrow-band sonar transducer. The frequency influence factor α_i is the frequency influence factor corresponding to the i-th sonar transducer. If the frequency influence factor α_i is high, it means that the acoustic signal generated by the sonar transducer of this frequency can detect the rock wall target more accurately and effectively. If the frequency influence factor α_i is low, it means the sonar energy conversion of this frequency and the acoustic signal produced by the instrument has little contribution to the accurate and effective detection of rock wall targets.

3.3 Determination of sonar detection object

In the traditional drilling sonar detection technology, the size of the cavity contour is calculated mainly according to the relationship between the detection distance and the travelling time and speed of the sound wave. When the sound wave travels between the sonar probe and the cave wall, it needs to go through the electrical/acoustic and acoustic/electrical conversion. Because of the energy conversion, the transmission circuit and timing control circuit, the transmission time will be associated with measurement errors, which is difficult to determine the propagation time of sound wave with high accuracy. The accuracy of the propagation time will directly affect the measurement accuracy of the cavity shape, which can be avoided by using the spectrum acoustic ranging method.

Suppose that the acoustic signal detected by the sonar is $u(0,t)$, the signal changes to $u(x,t)$ after the propagation distance, x, and time, t, and the ultrasonic signal at this time is $u(x,t)$. The signal is Fourier transformed[15-16], and its expression is

$$F[u(x,t)] = F[u(0,t)] \cdot \exp[-\mathrm{i}kx] \cdot \exp[-\partial x] \tag{6}$$

where $F[u(0,\ t)]$ is the Fourier transform of $u(0,t)$; k is the velocity of sound wave; ∂ is the attenuation coefficient of sound wave in the propagation medium.

When the propagation distance of sound wave is L, the signal of sound wave is $u(L,t)$. When the sound wave passes through the propagation medium and reaches the side near the propagation medium, the sound wave transmits and reflects.

Among them, the acoustic wave reflected in the propagation medium will reflect again in the propagation medium after encountering the sonar probe, that is, multiple reflections and transmissions are formed in the propagation medium. The reflected acoustic wave S can be expressed as

$$S=\sum_{e=0}^{\infty}u[L(2e+1),t] \tag{7}$$

where e is the number of reflections, and its Fourier transform is

$$F(S)=F[u(L,t)]\sum_{n=0}^{\infty}\{\exp[-i2kLe]\exp[-2\partial Le]\} \tag{8}$$

Let $z=\exp[-2\mathrm{i}kL]\exp[-2\partial L]$, the sound attenuation coefficient $\partial>0$, so that $|z|<1$, and the cumulative term of equation (8) can be reduced to

$$\sum_{n=0}^{\infty}\exp[-2\mathrm{i}kLe]\exp[-2\partial Le]=\lim_{n\to\infty}(1-z^n)/(1-z)=(1-z)^{-1} \tag{9}$$

According to the definition of wave number $k=\omega/C$, where ω is the angular frequency of sound wave; C is the speed of sound. Substituting relation (9) into relation (8), we can obtain

$$F(S)=F[u(L,t)][1-\exp(-2\mathrm{i}L\omega/C-2\partial L)]^{-1} \tag{10}$$

If the distance L between the sonar probe and the rock wall is a fixed value, the following relationship can be obtained:

$$2L\omega/C=2\pi m \tag{11}$$

where m is the number of echo pulses.

Eq. (11) shows that the amplitude spectrum of the reflected wave has a maximum value. In the amplitude spectrum, if the frequency corresponding to the maximum value is recorded as f_{m}, and the frequency corresponding to the amplitude maximum value adjacent to frequency f_{m} is recorded as f_{n}, then the frequency difference corresponding to the maximum value range is $f_0=|f_{\mathrm{m}}-f_{\mathrm{n}}|$.

In Fig.2, the maximum value point F_i of echo signal is selected, and its coordinates are expressed as (f_i, d_i). The two adjacent near-maximum points on the left side of maximum value point F_i are F_{i-1} and F_{i-2}, and the corresponding coordinates are expressed as (f_{i-1}, d_{i-1}), (f_{i-2}, d_{i-2}). The two adjacent near-maximum points on the right side of maximum value point F_i are F_{i+1} and F_{i+2}, and the corresponding coordinates are expressed as (f_{i+1}, d_{i+1}), (f_{i+2}, d_{i+2}). The line formed by connecting F_{i-2} and F_{i-1} is T_{i-2}, and its slope is expressed as k_{i-2}. The line formed by connecting F_{i-1} and F_i is T_{i-1}, and its slope is expressed as k_{i-1}. The line formed by connecting F_i and F_{i+1} is T_{i+1}, and its slope is expressed as k_{i+1}. The line formed by connecting F_{i+1} and F_{i+2} is T_{i+2}, and its slope is expressed as T_{i+2}. The slope of the four lines is expressed as

$$\left.\begin{aligned}k_{i-2}&=\frac{d_{i-1}-d_{i-2}}{f_{i-1}-f_{i-2}}\\k_{i-1}&=\frac{d_i-d_{i-1}}{f_i-f_{i-1}}\\k_{i+1}&=\frac{d_{i+1}-d_i}{f_{i+1}-f_i}\\k_{i+2}&=\frac{d_{i+2}-d_{i-1}}{f_{i+2}-f_{i-1}}\end{aligned}\right\} \tag{12}$$

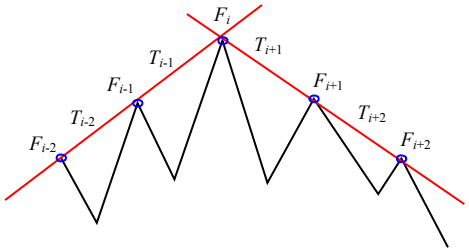

Fig.2 Schematic diagram of partial point coordinates of amplitude spectrum

According to relation (12), the distance L between sonar probe and rock wall can be calculated as

$$L=\frac{(k_{i-2}+k_{i-1}+k_{i+1}+k_{i+2})}{2\times4} \tag{13}$$

In order to better adapt to the detection environment, it is necessary to comprehensively consider and analyze the transmission signal and echo signal generated by multiple narrow-band sonar transducers with different natural frequencies. On the basis of introducing the frequency influence factor, the signal of multiple transducers can be synthesized and processed. Assuming that the transmission signal of the i-th frequency transducer is $u_i(0,t)$, after considering the influence factors of different frequencies, the frequency influence factors are stacked to be synthetically processed. The synthetic signal of sonar emission at cave depth h and of scanning angle θ can be expressed as $U(0,t)|_{h,\theta}$, where:

$$U(0,t)|_{h,\theta}=\sum_{i=1}^{n}\alpha_i|_{h,\theta}\cdot\lambda_i|_{h,\theta}\cdot u_i(0,t)|_{h,\theta} \tag{14}$$

In formula (14), the frequency influence factor of the i-th frequency transducer at cave depth h and scanning angle θ is $\alpha_i|_{h,\theta}$, the transmitted signal is $u_i(0,t)|_{h,\theta}$, and $\lambda_i|_{h,\theta}$ is the transmission gain adjustment coefficient, so as to ensure that the gains of different signals are of the same value.

Assuming that the echo signal of the i-th frequency transducer is $u_i(x,t)$, after considering the influence factors of different frequencies, the composite processing of superimposed frequency influence factors can be performed. The composite signal of sonar echo at cave depth h and scanning angle θ can be expressed as $U(x,t)|_{h,\theta}$:

$$U(x,t)|_{h,\theta}=\sum_{i=1}^{n}\alpha_i|_{h,\theta}\cdot\lambda_i|_{h,\theta}u_i(x,t)|_{h,\theta} \tag{15}$$

In formula (15), the frequency influence factor of the i-th frequency transducer at cave depth h and scanning angle θ is $\alpha_i|_{h,\theta}$, the echo signal is $u_i(0,t)|_{h,\theta}$, and $\lambda_i|_{h,\theta}$ is the gain adjustment coefficient, so as to ensure that the gains of different signals are of the same value.

According to eq. (13), the distance $\hat{L}$ between sonar probe and rock wall can be calculated as

$$\hat{L}=\frac{1}{8}\left(\frac{\hat{d}_{i-1}-\hat{d}_{i-2}}{\hat{f}_{i-1}-\hat{f}_{i-2}}+\frac{\hat{d}_i-\hat{d}_{i-1}}{\hat{f}_i-\hat{f}_{i-1}}+\frac{\hat{d}_{i+1}-\hat{d}_i}{\hat{f}_{i+1}-\hat{f}_i}+\frac{\hat{d}_{i+2}-\hat{d}_{i-1}}{\hat{f}_{i+2}-\hat{f}_{i-1}}\right)\Big|_{h,\theta} \tag{16}$$

In formula (16), the coordinates of the maximum-value

point of the sonar echo synthetic signal at cave depth h and scan angle θ are expressed as $(\hat{f}_i, \hat{d}_i)$, the coordinates of the two adjacent near-maximum points on the left side of the maximum point are expressed as $(\hat{f}_{i-1}, \hat{d}_{i-1})$ and $(\hat{f}_{i-2}, \hat{d}_{i-2})$ respectively, and the coordinates of the two adjacent near-maximum points on the right side of the maximum point are expressed as $(\hat{f}_{i+1}, \hat{d}_{i+1})$ and $(\hat{f}_{i+2}, \hat{d}_{i+2})$ respectively.

3.4 Construction of cavity shape

After calculating the sonar detection distance of a single detection point, the full circle contour scanning of the horizontal section at a certain depth can be realized by superposing the azimuth signals. The horizontal section contour at a certain depth can be formed by linear interpolation between the points. The three-dimensional shape of the cavity can be formed by meshing the points on the contour line of each horizontal section in the vertical direction according to the triangular mesh model. In the construction of cavity shape, this paper uses the synchronous triangle network model to reconstruct the mesh.

Firstly, connect the points on the two adjacent contour lines as synchronously as possible, and use Φ to represent the weighted value of the line segment on the contour line. It is calculated as the length of the line segment divided by the total length of the contour line, that is, the proportion of the line segment to the contour line. In Fig. 3, the triangle mesh model is defined as: suppose Φ_A represents the sum of the calculated weights on the contour Q_{h+n_h}, Φ_B represents the sum of the calculated weights on the contour $Q_{h+(n_h+1)}$. If the contour Q_{h+n_h} and contour $Q_{h+(n_h+1)}$ are connected to point $P_{h+n_{h,j},i}$ and point $P_{h+(n_{h,i}+1),i}$, and the weighted vlaues of line segments $Q_{h+n_{h,i},i}$ and $Q_{h+(n_{h,j}+1),i}$ are φ_A and φ_B respectively, then the corresponding relationships in the next step are $P_{h+n_{h,j},i}$ $P_{h+(n_{h,i+1}+1),i+1}$ and $P_{h+(n_{h,j}+1),i}$ $P_{h+n_{h,j+1},i+1}$. If $|\Phi_A + \varphi_A - \Phi_B| < |\Phi_B + \varphi_B - \Phi_A|$, select $P_{h+(n_{h,j}+1),i} \bullet P_{h+n_{h,i+1},i+1}$, i.e. one step in direction A. Otherwise, select $P_{h+n_{h,j},i}$ $P_{h+(n_{h,j+1}+1),i+1}$, one step in direction B.

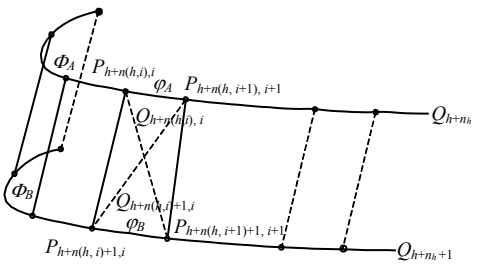

Fig.3 Triangular mesh model

According to the above triangle mesh model, triangular connections can be made to the points on the contour lines of the horizontal sections in each detection direction to form a more precise cavity three-dimensional shape diagram, as shown in Fig.4.

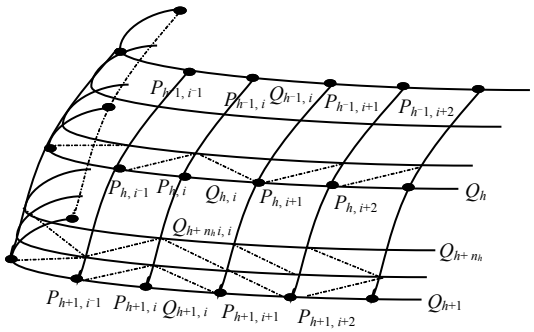

Fig.4 Schematic diagram of triangular meshing of cavity

4 Engineering application

There distribute karst and large-scale fracture zones along the planned subway lines in the northern China having adverse geological problems. In order to further investigate and analyze the distribution, burial depth and development of the karst caves, special geological exploration work has been carried out where the karst cave detection method based on multi-frequency borehole sonar proposed in this paper is applied.

4.1 Detection system

To serve the cavity detection method based on multi-frequency drilling sonar, a cavity detection system based on multi-frequency drilling sonar is developed. The system hardware is mainly composed of three parts: probe, communication cable and ground system. The probe is mainly responsible for information collection in the cavity. The communication cable is mainly responsible for real-time communication and data transmission between the probe and the ground system. The ground system is responsible for sending industrial control instructions to the probe in the dissolution chamber, as well as storage, presentation and calculation of data. The physical figure of the whole system is shown in Fig.5.

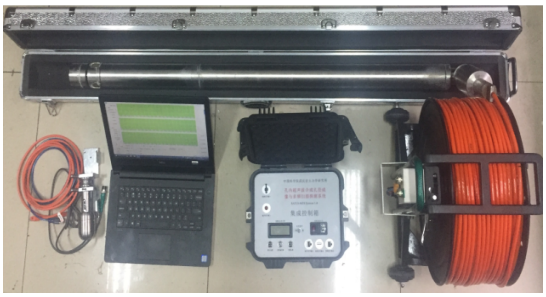

Fig.5 Multi-frequency sonar detection system

The probe is mainly composed of three ultrasonic transducers, motor control module, sensing module, main control circuit, power module and transmission module. The communication cable is made of optical fibre. The ground system is mainly composed of four parts including depth encoder, cable winch, control box, memory and data processor. The sensing module includes electronic compass, pressure

sensor, temperature sensor, motor angle encoder. The fixed working frequencies of the three ultrasonic transducers are different, which are 1 MHz, 500 kHz and 200 kHz, respectively. The three ultrasonic transducers are evenly distributed in the same horizontal section with an interval of 120°.

4.2 Data analysis

In this engineering application, three ultrasonic transducers simultaneously scan and detect the cavity in the entire borehole and a significant amount of detection data has been obtained. In the subsequent analysis and processing, the method described in this paper is used to describe the shape and size of the cavity.

Firstly, before scanning each section, the 200 kHz ultrasonic transducer carries out a distance prediction detection, that is, transmitting and receiving the echo signal from the cave wall, estimating the distance between the sonar probe and the corresponding cave wall by analyzing the 200 kHz acoustic signal, then calculating the best working frequency needed for the detection point according to relationship (4). Secondly, according to relationship (5), the frequency influence factors corresponding to three ultrasonic transducers at the detection point are calculated. Finally, the three echo signals are synthesized according to relationip (15). On the basis of the spectrum acoustic ranging method, the distance between the sonar probe and the rock wall at the detection point can be calculated according to the iterative relationship (16) after considering the influence factors of different frequencies. Subset of data obtained at a certain depth are shown in Table 1.

Table 1 Subset of data

Position /(°)	Estimated distance /mm	Optimum frequency /kHz	Frequency influence factor		
			1 MHz	500 kHz	200 kHz
0.0	2 000	731	0.37	0.39	0.24
10.0	2 500	630	0.30	0.43	0.27
20.0	2 300	666	0.33	0.41	0.26
⋮	⋮	⋮	⋮	⋮	⋮
330.0	1 500	885	0.45	0.34	0.21
340.0	1 600	848	0.43	0.35	0.22
350.0	1 900	756	0.38	0.38	0.24

After calculating the distance between a single sonar probe and the rock wall at the detection point, the profile of the section is reconstructed by linear interpolation on the horizontal section through superimposing the horizontal orientation and depth information obtained at the detection point inside the cave. The reconstruction of the three-dimensional shape grid of the cavity is realized by using the synchronous triangle network model described in this paper. The results are shown in Fig. 6. In order to more intuitively display the 3D features of the cave, it can match the optical cave images as shown in Fig.7.

4.3 Result contrast

To verify the feasibility of the cave detection method based on multi-frequency borehole sonar proposed in this paper, it is necessary to compare the results with the corresponding geological data to verify whether there exists cave phenomenon in that location of the borehole. The core map of the site is shown in Fig.8. According to the field drilling data and core map, there are karst caves in that section of the borehole filled with no other media but only water. Through comparison, the feasibility of the proposed method based on multi-frequency borehole sonar is verified, and the karst area in the borehole can be detected effectively.

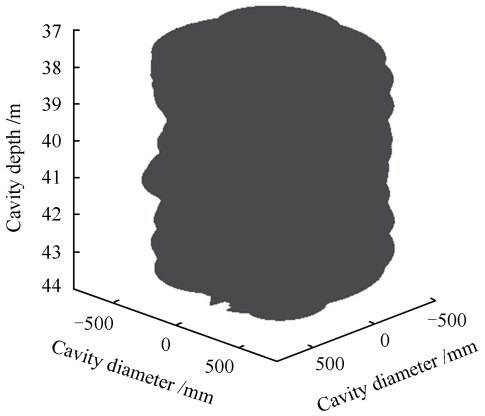

Fig.6 Cavity profile

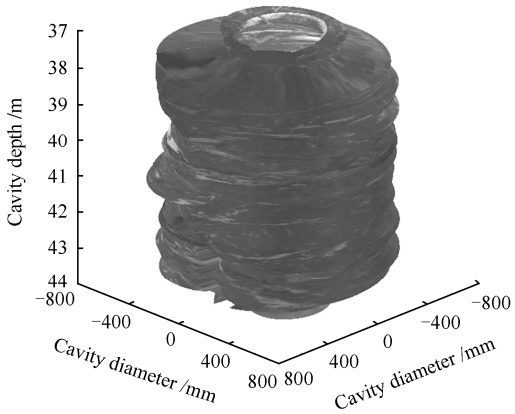

Fig.7 Cavity stereogram

Fig.8 On-site core image

In order to verify that the cave detection method based on the multi-frequency borehole sonar proposed in this paper is superior to the traditional borehole sonar method, the results obtained by applying the proposed method and the traditional methods are compared. In the comparison of the horizontal section profile, the data obtained from the 200 kHz ultrasonic

transducer is used as the comparison data to the traditional borehole sonar method, and the results are shown in Fig.9. It can be seen from the figure that, with the method proposed in this paper, the contour curve is smoother, and the fluctuation is smaller, which is more in line with the actual situation.

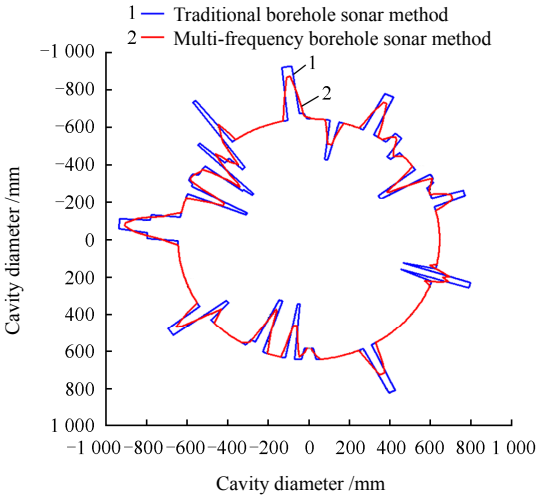

Fig.9 Horizontal profile contrast diagram

After the comparison of the horizontal profile, the three-dimensional shape of the reconstructed cavity is compared. The comparison results are shown in Fig.10 and Fig.11. In which, Fig.10 is the three-dimensional shape map calculated and reconstructed by the traditional sonar method, and Fig. 11 is the three-dimensional shape map reconstructed based on the multi-frequency sonar method. From Fig. 10, it can be observed that the data obtained from the traditional drilling sonar method fluctuates greatly, and the edges and corners of the reconstructed cavity diagram after interpolations and fittings are sharp. On the other hand, Fig. 11 shows that the data obtained from the multi-frequency sonar method fluctuates less, and the edges and corners of the diagram after interpolations and fittings are smooth.

By comparing Fig. 10 with Fig.11, we can see that the cavity shape reconstructed by the multi-frequency sonar method is more similar to the actual cavity shape than that reconstructed by the traditional sonar method, and the detection data is more stable. The main reason is that the multi-frequency sonar method synthesizes the detection data of multiple detection frequencies, and considers the contribution of different frequencies to the actual detection object by using the parameters of frequency influence factor. So that the influence of different frequencies on the detection result analysis is reflected in priority during the analysis of the detection data in combination with the best real-time frequency. This effectively avoids the contradiction between detection scale and detection accuracy, and allows the detection system to be applied more accurately and broadly in the detection of different underground cavities with various shapes and sizes. The proposed method can provide effective data support for engineering construction in karst area.

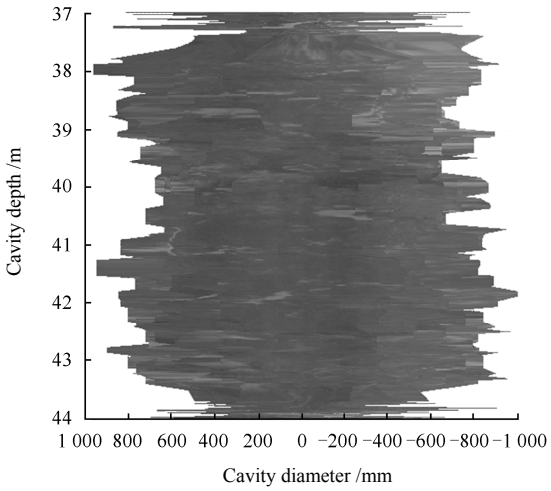

Fig.10 Reconstruction of cavity based on traditional sonar

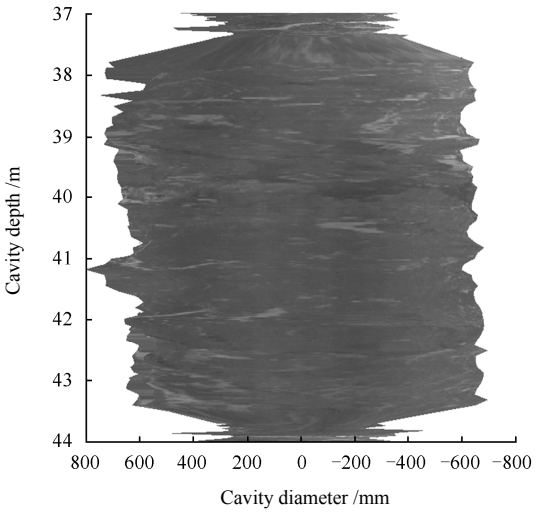

Fig.11 Reconstruction of cavity based on multi-frequency sonar

5 Conclusions

(1) The optimum frequency function provides reference for the selection of the best working frequency of the detection system.

(2) The parameter of frequency influence factor effectively describes the deviation between the natural frequency and optimal frequency.

(3) The spectrum acoustic ranging method effectively avoids the influence caused by the propagation time error on the detection accuracy of cavity shape.

(4) The proposed multi-frequency sonar detection method is feasible and accurate, and the accuracy is higher than that achieved by the traditional borehole sonar method.

References

[1] DENG Chao-wen, ZHANG Xiu-jie, LI Hong-zhong. Distribution characteristics of carbonate rocks and related karst exploration methods in Guangdong province[J]. Science and Technology Innovation Herald, 2015(7): 76.

[2] LI Jian-peng, NIE Qing-ke, LIU Quan-sheng, et al. Risk assessment method of karst ground collapse based on weight back analysis[J]. Rock and Soil Mechanics, 2018, 39(4): 1395-1400.

[3] SHI Xiang-feng. Study on the roof stability of concealed karst cave under pile foundation loading in karst areas[D]. Beijing: Graduate University of Chinese Academy of Sciences, 2005.

[4] JIANG Shi-qing. Analysis of technical problems in karst area survey[J]. High-tech. Enterprises of China, 2017(12): 271-272.

[5] HU Chao-bin, DENG Shi-kun, WANG Bao-xun, et al. Application study of the GPR method in the detection of karsts beneath artificial excavated hole pile[J]. Journal of Geological Hazards and Environment Preservation, 2009(2): 74-78.

[6] CUI Zhi-sheng, XIA Cai-chu, ZHAO Kai. Discussion on the method and application of detection method for large diameter rock-socketed pile bottom cave[J]. Western China Communication Science and Technology, 2011(7): 46-50.

[7] GE Zu-huan, HU Chun-qing, XIANG Hui-min, et al. The exploration of limestone karst cave at the end of pile[J]. Geophysical and Geochemical Exploration, 2004, 28(1): 85-87.

[8] LIAN Guang-wei. Research on the detection technology of cave on the bottom of the cast-in-place pile[D]. Chongqing: Chongqing Jiaotong University, 2012.

[9] ZHANG Zhang, SUN Tao, LIU Ji-dong, et al. Frequency domain analysis of ground penetrating rader in detecting the karst rock cavity under pile tips[J]. Soil Engineering and Foundation, 2014(2): 163-166.

[10] LIU Wen-feng, ZHANG Zhen-yong. The application of ground-penetrating radar to the karst foundation investigation[J]. Geophysical and Geochemical Exploration, 2014, 38(3): 624-628.

[11] CHEN Jian-hua. Research on the construction technology of the deep pile foundation in the strong karst development area[D]. Changsha: Central South University, 2014.

[12] ZHAO Jie. Research of tube wave prospecting karst development under large diameter pile[D]. Qingdao: Ocean University of China, 2012.

[13] LI Bin, FAN Qiu-yan, QIN Feng-rong. Stability analysis of karst cave roof in karst area[J]. Chinese Journal of Rock Mechanics and Engineering, 2002, 21(4): 532-536.

[14] WANG Jin-chao, WANG Chuan-yin, TANG Xin-jian. A method for determining empty area profile based on borehole ultrasonic scanning technique[J]. Journal of Yangtze River Scientific Research Institute, 2018, 35(3): 104-109.

[15] LIU Xue-feng, LI Shu-guang, LI Shu-bang. Spectral analysis technology for measuring the sound velocity of ultrasound[J]. Journal of Qingdao University (Natural Science Edition), 2006, 19(11): 3-5.

[16] LIU Yan-ping, WANG Yin-guan. Acoustic velocity measurement by pulse echo spectrometry[J]. Technical Acoustics, 2008, 27(5): 176-177.